Journal of Power Sources 247 (2014) 78–83

Contents lists available at ScienceDirect

Journal of Power Sources

journal homepage: www.elsevier.com/locate/jpowsour

Magnetic sputtered amorphous Si/C multilayer thin films as anode materials for lithium ion batteries

Yongfeng Tong [a], Zhuang Xu [a], Chang Liu [a], Guang'an Zhang [b], Jun Wang [a,*], Z.G. Wu [a]

[a] School of Physical Science and Technology, Lanzhou University, Lanzhou 730000, China
[b] State Key Laboratory of Solid Lubrication, Lanzhou Institute of Chemical Physics, Chinese Academy of Sciences, Lanzhou 730000, China

HIGHLIGHTS

- The amorphous silicon/carbon multilayer thin films were synthesized by magnetic sputtering.
- The Si/C multilayer films displayed a good cycling performance and structure stability.
- The micro-scale films displayed a good long cycling performance.
- The effects of the amorphous carbon layers to the cycling performance were discussed.

ARTICLE INFO

Article history:
Received 5 May 2013
Received in revised form
2 August 2013
Accepted 21 August 2013
Available online 31 August 2013

Keywords:
Magnetic sputtering deposition
a-Si/C multilayer thin films
Electrochemistry
Lithium-ion battery anode

ABSTRACT

We have successfully synthesized the amorphous silicon/carbon (a-Si/C) multilayer thin films by magnetic sputtering method. The bonding characteristics and phase identification were investigated by X-ray diffraction (XRD) and Raman spectrum. The electrochemical performance of the a-Si/C multilayer thin films as anode materials for lithium ion batteries showed that with various thicknesses of Si layers, the electrodes displayed huge differences on the reversible capacity and cycling stability. The 500 nm a-Si/C multilayer films, with the thickness ratio d_{Si}:d_C = 5:1, displayed a high reversible capacity of about 2000 mA h g^{-1} over 200 cycles at 1C rate and a best structure integrity at various charging/discharging rates test. The micro-scale a-Si/C multilayer thin films (1.1 μm) also showed a good cycling performance with a capacity of about 1900 mA h g^{-1} at a current density of 2000 mA g^{-1} over 200 cycles.

1. Introduction

The commercial graphite anode is widely used in lithium ion battery due to its stable cycling performance [1]. But its drawback is also obvious. The relatively low specific capacity (372 mA h g^{-1}) [2] is not suitable for high power and high energy density lithium ion batteries [3]. Among the candidates [4–6], silicon, with its highest theoretical specific capacity (4200 mA h g^{-1}; $Li_{22}Si_5$), is considered as the most potential one to meet the demands of high performance lithium ion batteries (LIB). Despite the high power and high energy density nature, silicon suffers from a huge volume expansion (~310%; $Li_{22}Si_5$) [7] during the intercalation and de-intercalation of Li^+, resulting in poor capacity retention, high initial cycle irreversible loss and low columbic efficiency [8]. Hence many efforts have focused on addressing the drawbacks and of all the solutions, to synthesize nanostructure anodes is a feasible approach to minimize the volume expansion effects, and many researches have demonstrated that nano-scale silicon together with the carbon buffer can significantly improve the electrochemical performance of the Si-based electrode, including the carbon coated Si nanowires [9–11], Si nanoparticles [12–14], Si/C nanocomposite [15,16], Si/C nanotubes [17,18], porous Si structure [19–21] and Si/C nanofilms [22,23] electrodes, et al.

As well as the high capacity retention, the better structure stability of Si electrode also plays an important role in the electrochemical performance. In our previous work, the a-Si/C multilayer thin films showed a good electrochemical performance during the test [24]. In this work, we studied the appropriate thickness ratio of Si/C (d_{Si}/d_C) in 30 nm periodic thickness multilayer a-Si/C films that showed best structure stability and high capacity retention during

* Corresponding author.
E-mail address: wangj-phy@lzu.edu.cn (J. Wang).

0378-7753/$ – see front matter © 2013 Elsevier B.V. All rights reserved.
http://dx.doi.org/10.1016/j.jpowsour.2013.08.087

the long cycling. Thin film deposition technology provides a good way to accurately control the thickness of the films and allows the study of the nano-size effects on electrochemical performance of the a-Si/C films.

2. Experimental procedure

2.1. Materials preparation

The a-Si/C multilayer films were prepared in a high vacuum chamber equipped with two sources: ratio frequency (RF) magnetic sputtering of a silicon target and direct current (DC) magnetic sputtering of a carbon target. The copper foil and silicon substrates were placed 10 cm away from the Si and C targets. The two sources were driven simultaneously and separately to ensure that they can alternately work during the deposition process. The sputtering powers for Si target and C target were both 300 W. The vacuum chamber was pumped to 2.0×10^{-3} Pa by a molecular pump and the deposition of both Si and C layers was proceeded in pure Ar with a working pressure of 1 Pa. The deposition rates calculated from total film thickness were 5.8 nm min^{-1} for carbon and 18.0 nm min^{-1} for silicon. So the thickness of Si and C layer in one periodic layer and the total thickness of the film could accurately be controlled by the deposition time. Before the deposition of a-Si/C multilayer films, a 50 nm Ti thin film was deposited as the intermediate layer and the C layer of the a-Si/C multilayer films was first deposited on the Ti layer to get a relatively better adhesive strength. At the end, an about 15 nm carbon layer was deposited on the top of the films to avoid the oxidation of Si.

2.2. Characterization and electrochemical measurement

The a-Si/C multilayer films were characterized by scanning electron microscopy (SEM), X-ray diffraction (XRD), Raman spectrum and X-ray photoelectron spectroscopy (XPS). The a-Si/C multilayer films deposited on copper foils were directly used as the electrode for lithium ion batteries and the lithium metal was used as the counter electrodes. 1 M $LiPF_6$ in ethylene carbonate (EC)/dimethyl carbonate (DMC) was utilized as the electrolyte, and the EC/DMC = 1:1 in volume. The half-cell was assembled in a glove-box filled with pure Argon (99.99%) in the presence of an oxygen scavenger and a sodium drying agent. Cyclic voltammetric measurements were performed on LAND CR2016 battery test system in the voltage range of 0.01–1.2 V at a scan rate of 0.1 mV s^{-1}. The electrochemical impedance spectroscopy (EIS) measurement was conducted on a CHI600E Electrochemical Workstation in the frequency range from 10^{-3} Hz to 10^{5} Hz. The alternating amplitude was 5 mV.

3. Results and discussion

In this work, the carbon layer deposited in all the samples was 5 nm in thickness. The relatively thin C layer can significantly improve the stability of the electrode without high capacity reduction. And the effect of the various thickness of the Si layer on the electrochemical performance as the anode for lithium ion battery (LIB) was investigated. As has been illustrated in Table 1, Sample A, B and C corresponded to films with different silicon and carbon thickness ratios (d_{Si}/d_C) but with the same total film thickness (t_T). Sample A, D and E contained the same d_{Si}/d_C but different t_T. Sample F and G was the pure Si film with a film thickness of 500 nm and 350 nm, respectively. 350 nm equaled to the content of Si in the multilayer Sample A.

Fig. 1(a) and (b) was the planar and the cross-section SEM of the multilayer sample, respectively. The boundaries between the Si and C layers could be clearly observed. Fig. 1(c) was the low-angle X-ray diffraction patterns (LAXRD). From the LAXRD, the modulate period of the multilayer film was calculated with the modified Bragg formulas:

Table 1
Sample A–F with different thickness ratios (d_{Si}/d_C) and different film thicknesses (t_T). Sample A, B and C have different d_{Si}/d_C but the same t_T. Sample A, D and E have the same d_{Si}/d_C but different t_T. F and G were the pure Si film with the thickness of 500 nm and 350 nm, respectively.

Sample	A	B	C	D	E	F	G
d_{Si}/d_C	5:1	6:1	7:1	5:1	5:1	Pure silicon	Pure silicon
t_T	500 nm	500 nm	500 nm	1100 nm	1300 nm	500 nm	350 nm

$$d = \lambda_{Cu}/2\sqrt{\left[(n+1)^2 - n^2\right]/(\sin^2\theta_{n+1} - \sin^2\theta_n)}$$

The wavelength of the incident X-ray $\lambda_{cu} = 0.154$ nm, with the number of the LAXRD peaks (n) and angle (θ), the modulate period was calculated to be about 25 nm, which was consistent with the pre-determined modulation period.

The periodic structure was further confirmed by the XPS depth profile in Fig. 1(d). Because of the different sputter rate for Si and C (silicon is relatively easier removed by sputtering than carbon), the XPS sputtering time didn't exactly correspond to the thickness ratio of Si and C from XPS spectrum. Fig. 1(e) showed the Raman spectrum of the a-Si/C multilayer thin films. The transverse acoustic (TA) at 155 cm^{-1}, longitudinal optic (LA) at 310 cm^{-1}, transverse optic (TO) at 375 cm^{-1} and longitudinal optic (LO) at 485 cm^{-1} are the typical feature of amorphous Si vibration modes [22,25], the typical D (1360 cm^{-1}) and G (1580 cm^{-1}) [26] peaks of amorphous C were also detected. The results confirmed the multilayer thin films possess disordered amorphous phase but no significant amounts of crystalline Si or C. Analogous structure information can also be observed in XRD pattern in Fig. 1(f), the peaks that were identified corresponded to Cu diffraction from the copper substrate, no significant peaks corresponding to Si and C were observed, indicating the amorphous structure of Si and C.

Fig. 2(a) showed the cycling performance of the a-Si/C multilayer thin films at a current density of 2000 mA g^{-1} (1C for Sample A, F and G, 0.9C for Sample B and C, 0.5C for Sample D and E). Sample A with a $d_{Si}/d_C = 5:1$, gained a best cycling stability during the charge/discharge process. The specific capacity was about 2000 mA h g^{-1} after 200 cycles. As the d_{Si}/d_C increased, Sample B reached a capacity of about 3000 mA h g^{-1} at 130th cycle and then showed a slightly capacity decrease with the cycle numbers, which indicted that Sample B had higher capacity but lower stability than Sample A. Compared with Fig. 1(a), the SEM image after 200 cycles (Fig. 2(b)) showed the structural fracture and pulverization of the films. A dramatically capacity fading could be seen in Sample C, which predicted that under the high d_{Si}/d_C, the buffer effect of the C layer weakened by the large expansion of Si layers. Sample G (350 nm pure silicon sample) displayed a capacity failure after only 40 cycles, which indirectly confirmed the buffer effect of carbon in the multilayer samples. But due to the high ion conductivity induced by carbon additive, the insertion and extraction of Li^+ in Sample C was easier than that in the pure Si Sample F, thus deep Si layers of Sample C suffered the structural expansion at early cycles, leading to the fast structural breakdown during the charge/discharge process, which may explain the even poorer electrochemical performance of Sample C than the pure silicon Sample F. Sample A, D and E had the same d_{Si}/d_C ratio but different film thicknesses, and they all displayed high capacity retention and high coulombic efficiency of 1950 mA h g^{-1}, 99.7% for D and

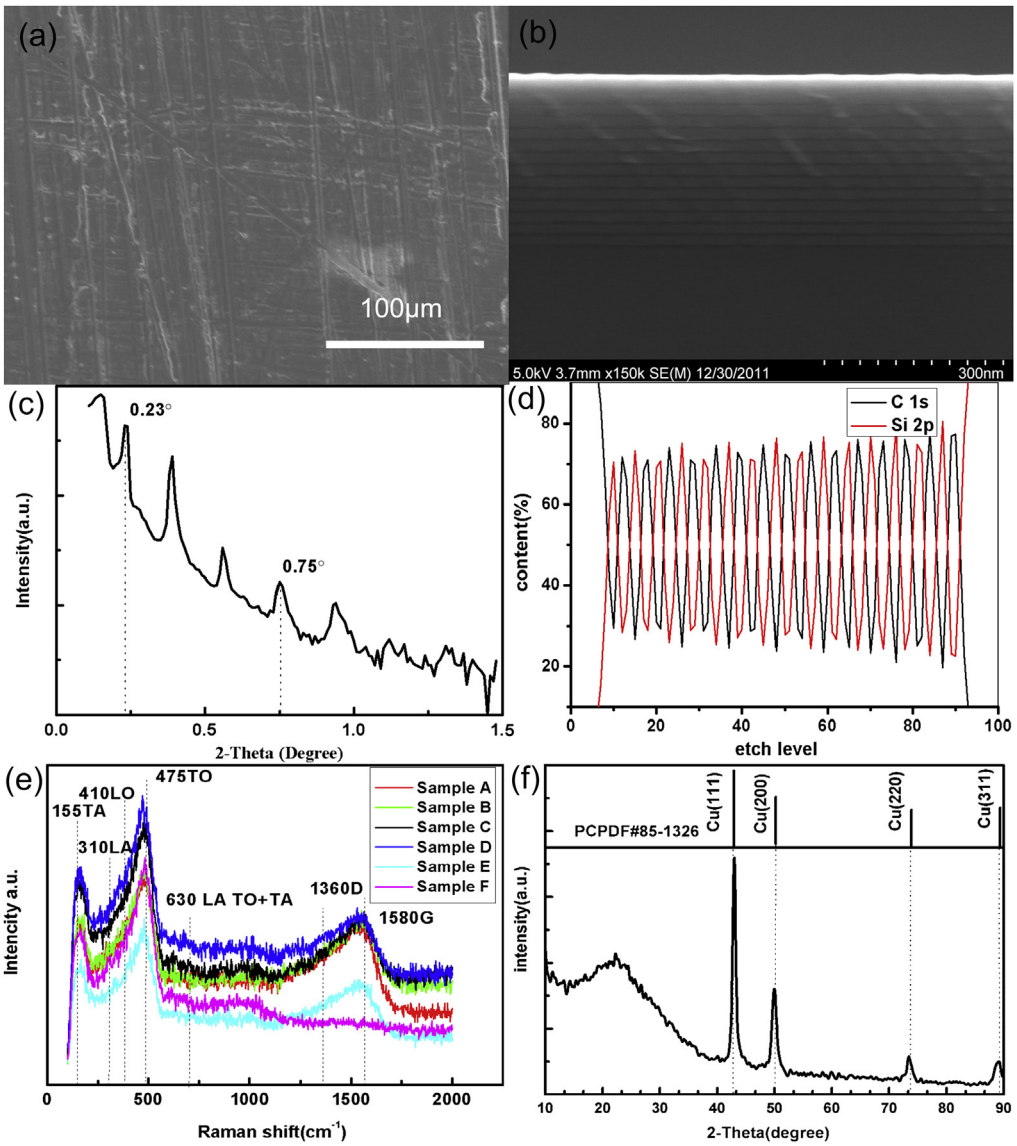

Fig. 1. (a), (b) The typical SEM image of the surface morphology and cross-section of Sample A, respectively; (c) the low angle X-ray diffraction of Sample A; (d) the XPS depth profile of the Sample A. (e) Raman spectrum of the a-Si/C samples and the pure silicon film; (f) XRD pattern of the a-Si/C multilayer thin films of the a-Si/C multilayer films Sample A.

1800 mA h g^{-1}, 99.6% for E after 200 cycles. What we should note was that the D and E were micro-scale thin films, the increased Li diffusion length and large stress induced by Li insertion/extraction would usually lead to poor cycling performance as reported. Our results showed good structure integrity and high capacity retention of the micro-scale a-Si/C multilayer thin films than ever reported in literature [27–29], indicating the promising application of the micro-scale a-Si/C films as the anode for lithium ion batteries. Sample D underwent a long activation of 150 cycles, which was not suitable for practical use. The short active time of Sample E but long active time of Sample D may be due to the defects inside the films. Thicker Sample E tended to gain more defects due to the high internal stress, which allowed Li^+ to better diffuse into and intercalate inside the films during the charge/discharge process, leading to a short active time [30]. The pure amorphous Si film Sample F (500 nm equal the t_T of Sample A) and Sample G (350 nm equaled the Si content in Sample A) acted as a comparison. The capacities of both samples were fading quickly with the cycles, indicating poor structure integrity of the pure Si film. The results showed that at a certain d_{Si}/d_C ratio of 5:1, the multilayer a-Si/C films gained best structure stability. The carbon buffer significantly accommodated the volume expansion of Si. With the increasing of d_{Si}/d_C, the thicker Si layer induced a huge stress that the carbon can hardly release during the cycles, leading to the pulverization and deterioration of the Si. Fig. 2(c) was the coulombic efficiency of the multilayer Sample A–G for the first 40 cycles. The coulombic efficiency of the multilayer a-Si/C samples were low in the beginning but quickly approached 99% in a few cycles for most of the samples. Because of the long active time, the coulombic efficiency of Sample D displayed a continuous increase during the first 40 cycles.

Fig. 2(d) was the cyclic voltammogram (CV) curve of Sample A. In the Li insertion part, a cathode peak at 0.18 V was seen, which can be ascribed to the formation of Li–Si alloys [31]. It exhibited an enhanced intensity from the 1st cycle to the 3rd cycle, which may be attributed to the gradual activation of the electrode. In the Li extraction part, two broad anodic peaks appeared at around 0.31 V and 0.55 V, corresponding to the phase transition between amorphous Li–Si alloys and amorphous Si [32–34].

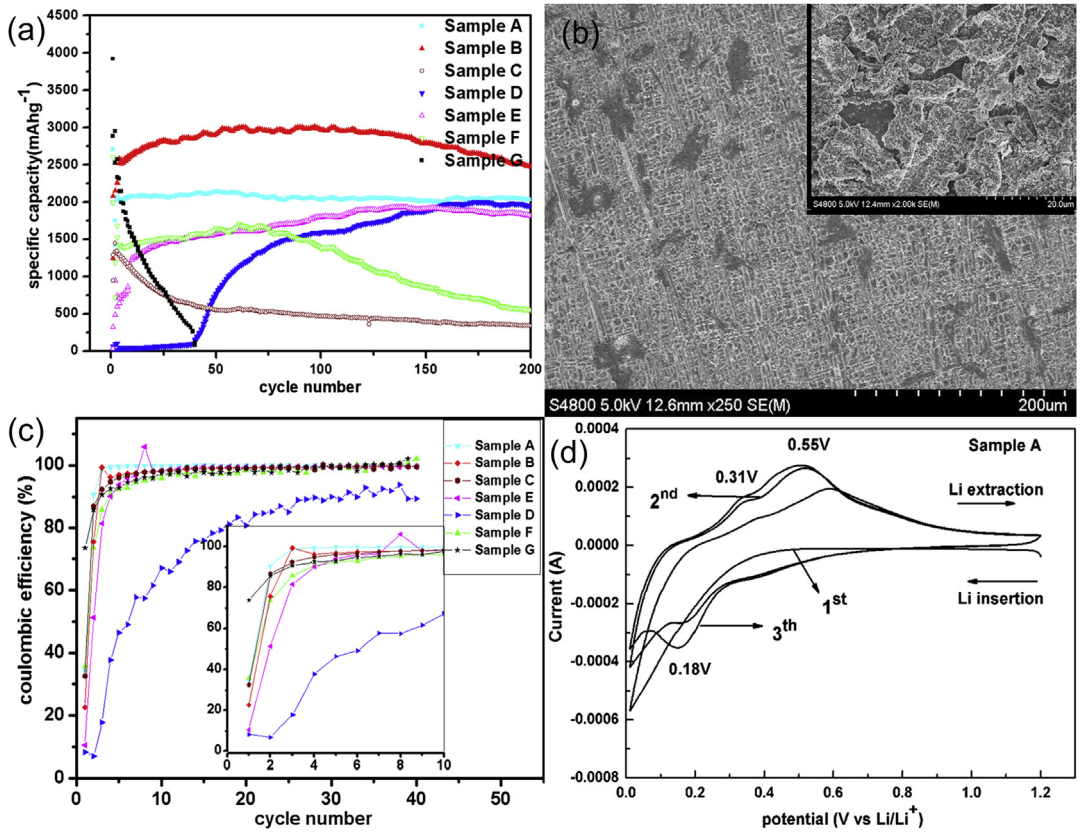

Fig. 2. (a) Charge/discharge capacity profiles of the a-Si/C multilayer thin films A–G and the pure Si film at a current density of 2000 mA g^{-1}. The capacity was calculated with respect to the total mass of carbon and silicon layers. The cur-off voltage range is 0.01 V–1.5 V; (b) the surface morphology of Sample B after 200 cycles, inset was the high resolution image of the films; (c) coulombic efficiency of the Sample A–F for the first 40 cycles. (d) Cyclic voltammogram curve of Sample A at a scan rate of 0.1 mV s^{-1}.

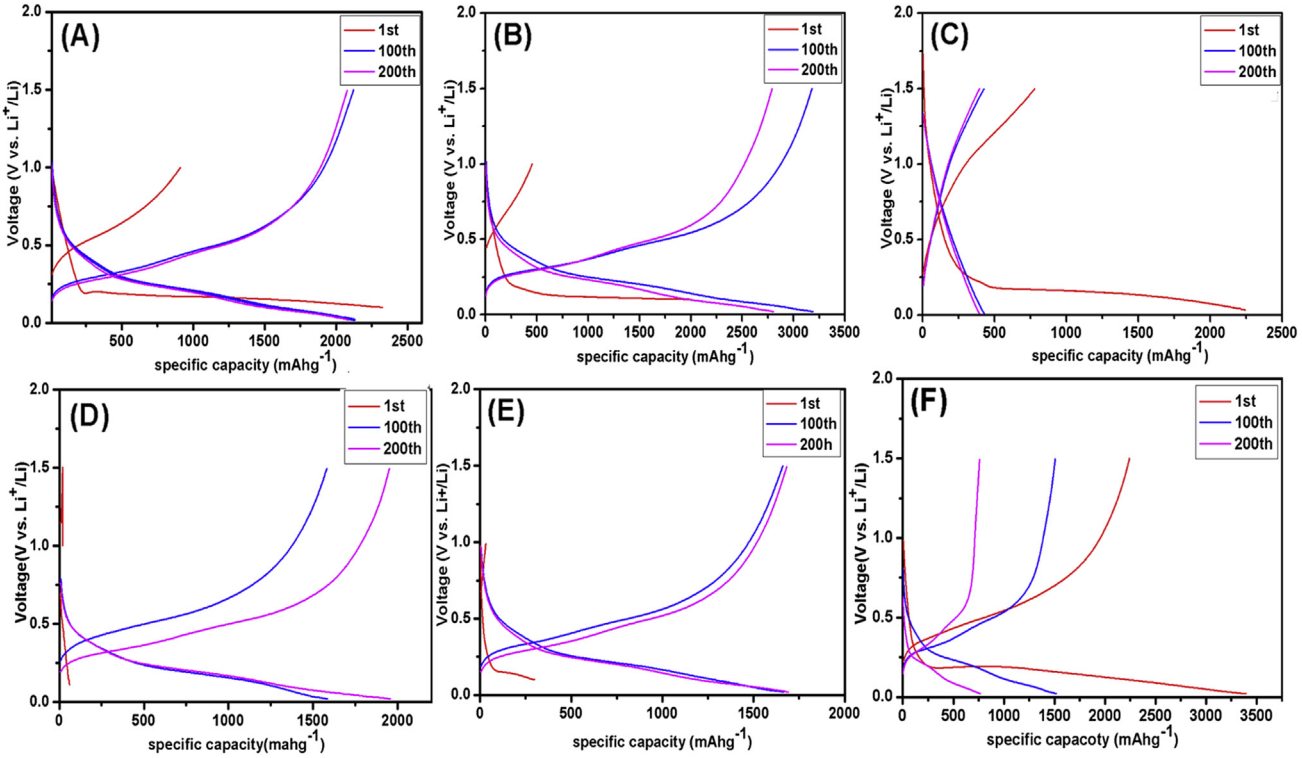

Fig. 3. Voltage profile of the 1st, 100th and 200th cycles for the a-Si/C multilayer thin films and the pure Si film. Applied current density was 2000 mA g^{-1} (1C rate). A–F corresponded to the Sample A to F, respectively.

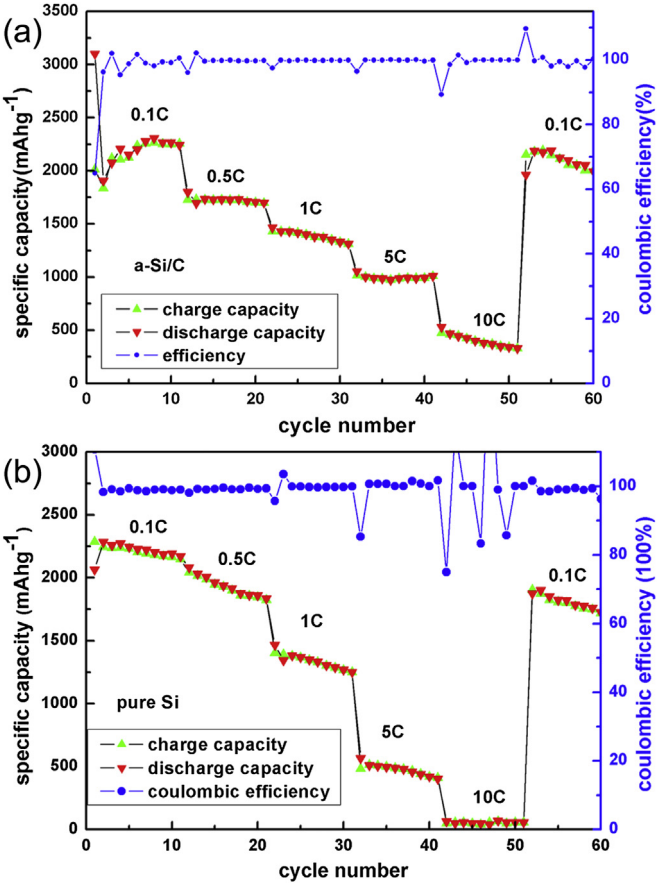

Fig. 4. The rate capability of (a) the a-Si/C multilayer thin films (Sample A) and (b) the pure Si film (Sample F) in the potential window between 0.01 V and 1.2 V.

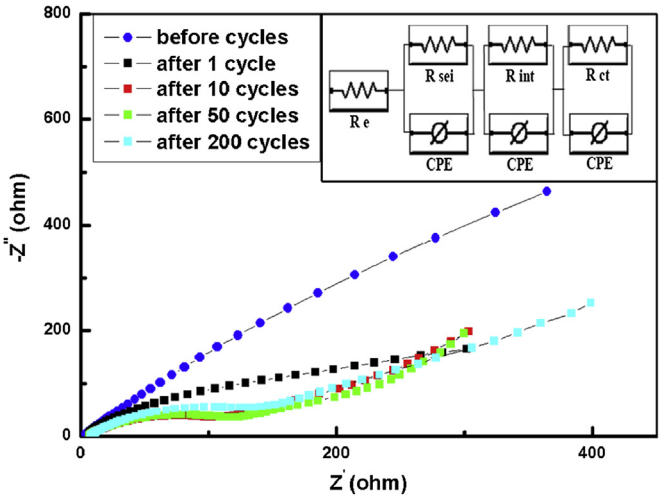

Fig. 5. Nyquist plots of the a-Si/C multilayer films Sample A before and after discharge/charge cycles. Inset was the equivalent circuit used to model the impedance spectra. (R_e) the ohmic resistance associated with the electrolyte and cell component; (R_{SEI}) the resistance of the SEI formation; (R_{int}) the interface electronic contact resistance relevant to resistance of electronic contact between active materials and current collector; (R_{ct}) the charge-transfer resistance for the electrode reaction.

Fig. 3 was the voltage profiles of the Sample A to F for the 1st, 100th and 200th cycles at 2000 mA g^{-1}, Sample G was not listed because of its short cycle life. For Sample A, B and D, the long plateau near 0.2 V in the discharge curve made the major contribution to the reversible capacity, indicating a stable intercalation process. And the discharge curves were much smoother than that of the pure silicon, indicating the multilayer structure significantly improves the stability of the electrode.

The excellent electrochemical performance of the a-Si/C multilayer thin films was attributed to the intermediate carbon layers by three features: firstly, the carbon layers act as a buffer as it has a relatively low volume expansion. The buffers have an opposing force against the volume expansion of Si during the lithiation, thus improving the structure integrity of the electrode. Secondly, the carbon additive can provide an excellent electronic contact with its high conductivity. And the defects in the amorphous carbon layers and the electric conduction pathway between the active and the cushion layers may also lead to easier transfer of the Li^+, resulting in the improvement of ion conductivity of the multilayer films electrode. Thirdly, it has been reported that the carbon coating on the Si can significantly improve the electrochemical performance by preventing the Si from directly contacting with the electrolyte [23] and suppressing the formation of the solid electrolyte interphase (SEI) [29,35–37]. But the initial capacity loss largely dependents on the crystallization of the carbon coating, which may explain the still relatively low initial coulombic efficiency in the multilayer samples [38]. And another effect of the upmost carbon layer was to avoid the oxidation of the silicon, as the SiO_2 had no Li^+ storage ability. But the drawback of the carbon additive is that the better capacity stability is at the expense of enlarging irreversible capacity and reducing the specific capacity.

The rate capabilities of the a-Si/C multilayer thin films and the pure Si film were compared in Fig. 4. Fig. 4(a) was the rates test of Sample A. At low current density of 200 mA g^{-1} (0.1C) and 1000 mA g^{-1}, the capacities of the a-Si/C multilayer films were 2200 mA h g^{-1} and 1700 mA h g^{-1}. And it delivered a high reversible capacity of 1500 mA h g^{-1}, 1000 mA h g^{-1} and 300 mA h g^{-1} at a current density of 2 A g^{-1}, 10 A g^{-1} and 20 A g^{-1}, respectively. When the current density returned to 200 mA g^{-1}, 95% of the initial capacity was obtained, indicating a good structure stability of the electrode. As a comparison, the pure silicon (Sample F) was also tested in Fig. 4 (b). But the reversible capacities at every current density were lower than that of the a-Si/C multilayer thin films (Sample A).

Electrochemical Impedance Spectroscopy was also employed to investigate the impedance properties of the a-Si/C multilayer films (Sample A) electrode before and after cycling in Fig. 5. And the spectrum was fitted well on an equivalent circuit shown in the inset of Fig. 5. The equivalent circuit consists of a series of tress resistors and constant phase elements (CPE) in parallel. R_e is the ohmic resistance associated with the electrolyte and cell component, R_{SEI} is the resistance of the SEI formation, R_{int} is the interface electronic contact resistance relevant to resistance of electronic contact between active materials and current collector, R_{ct} is the charge-transfer resistance for the electrode reaction. After the 1st, 20th, 50th and 200th cycles, the spectrums had similar features: one depressed semicircle in the high-to-medium frequency ranges and an incline line in the low frequency range. The diameter of the depressed semicircle represents the overlap between the resistance of SEI film and the charge-transfer resistance, and the inclined line corresponds to the diffusion of lithium ion [39,40]. It was reported that the diameter of the semicircle usually increased with cycling due to the gradual pulverization of the electrodes, resulting in a poor electronic contact [41]. The increasing diameter of the EIS spectrum in the first cycle was due to the pulverization of the electrode with the expansion of Si. In the following cycles, the relatively stable diameter of the semicircle indicated a stable contact between the electrode and the collector. No further pulverization occurred. The results further confirmed the buffer effect of the C layers successfully accommodated the volume expansion of

Si, leading to the structure stability and the improvement of the cycle-life of the a-Si/C multilayer films electrodes.

4. Conclusions

In this work, the a-Si/C multilayer films were prepared by alternatively deposited by magnetic sputtering of Si and C targets and the long-term cycling performance and rates tests were conducted as the anode electrode for lithium ion batteries. The a-Si/C multilayer films Sample A (d_{Si}/d_C = 5:1, t_T = 500 nm) electrode displayed a high specific capacity retention of 2000 mA h g^{-1} at 1C rate after 200 cycles, and a good structure integrity in the rates tests. The micro-scale a-Si/C multilayer thin film also reached a specific capacity of 1900 mA h g^{-1} even after 200 cycles. The results predicted the a-Si/C multilayer thin films to be a promising anode material for lithium ion battery.

Acknowledgment

This work was supported by the Basic Scientific Research Business Expenses of the Central University (lzujbky-2010-86) and the Open Project of Key Laboratory for Magnetism and Magnetic Materials of the Ministry of Education, Lanzhou University under award number LZUMMM2012014.

References

[1] W. Hongyu, Masaki Yoshio, J. Power Sources 93 (2001) 123.
[2] B. Scrosati, Electrochim. Acta 45 (2000) 2461–2466.
[3] J.P. Maranchi, A.F. Hepp, P.N. Kumta, Electrochem. Solid-State Lett. 6 (2003) A198.
[4] Z. Yang, D. Wang, F. Li, D. Liu, P. Wang, X. Li, H. Yue, S. Peng, D. He, Mater. Lett. 90 (2013) 4–7.
[5] X. Chen, J.P. Cheng, Q.L. Shou, F. Liu, X.B. Zhang, CrystEngComm 14 (2012) 1271.
[6] C.X. Guo, M. Wang, T. Chen, X.W. Lou, C.M. Li, Adv. Energy Mater. 1 (2011) 736–741.
[7] L.Y. Beaulieu, K.W. Eberman, R.L. Turner, L.J. Krause, J.R. Dahn, Electrochem. Solid-State Lett. 4 (2001) A137–A140.
[8] S.W. Lee, M.T. McDowell, J.W. Choi, Y. Cui, Nano Lett. 11 (2011) 3034–3039.
[9] Y. Liu, K. Huang, Y. Fan, Q. Zhang, F. Sun, T. Gao, L. Yang, J. Zhong, Electrochim. Acta 88 (2013) 766–771.
[10] C.K. Chan, H. Peng, G. Liu, K. McIlwrath, X.F. Zhang, R.A. Huggins, Y. Cui, Nat. Nanotechnol. 3 (2008) 31–35.
[11] K. Peng, J. Jie, W. Zhang, S.-T. Lee, Appl. Phys. Lett. 93 (2008) 033105.
[12] G. Zhao, L. Zhang, Y. Meng, N. Zhang, K. Sun, Mater. Lett. 96 (2013) 170–173.
[13] J.K. Lee, K.B. Smith, C.M. Hayner, H.H. Kung, Chem. Commun. 46 (2010) 2025–2027.
[14] J. Bae, J. Solid State Chem. 184 (2011) 1749–1755.
[15] M.-S. Wang, L.-Z. Fan, J. Power Sources (2013).
[16] Y.-X. Wang, S.-L. Chou, J.H. Kim, H.-K. Liu, S.-X. Dou, Electrochim. Acta 93 (2013) 213–221.
[17] Z. Wen, G. Lu, S. Mao, H. Kim, S. Cui, K. Yu, X. Huang, P.T. Hurley, O. Mao, J. Chen, Electrochem. Commun. 29 (2013) 67–70.
[18] H. Wu, G. Chan, J.W. Choi, I. Ryu, Y. Yao, M.T. McDowell, S.W. Lee, A. Jackson, Y. Yang, L. Hu, Y. Cui, Nat. Nanotechnol. 7 (2012) 310–315.
[19] Q. Shou, J. Cheng, L. Zhang, B.J. Nelson, X. Zhang, J. Solid State Chem. 185 (2012) 191–197.
[20] M.-S. Wang, L.-Z. Fan, M. Huang, J. Li, X. Qu, J. Power Sources 219 (2012) 29–35.
[21] M. Thakur, S.L. Sinsabaugh, M.J. Isaacson, M.S. Wong, S.L. Biswal, Scientific Rep. 2 (2012) 795.
[22] M.K. Datta, J. Maranchi, S.J. Chung, R. Epur, K. Kadakia, P. Jampani, P.N. Kumta, Electrochim. Acta 56 (2011) 4717–4723.
[23] Y.-N. Zhou, M.-Z. Xue, Z.-W. Fu, J. Power Sources 234 (2013) 310–332.
[24] J. Wang, Y. Tong, Z. Xu, W. Li, P. Yan, Y.-W. Chung, Mater. Lett. 97 (2013) 37–39.
[25] V. Baranchugov, E. Markevich, E. Pollak, G. Salitra, D. Aurbach, Electrochem. Commun. 9 (2007) 796–800.
[26] D. Liu, Y. Wang, Y. Xie, L. He, J. Chen, K. Wu, R. Xu, Y. Gao, J. Power Sources 232 (2013) 29–33.
[27] T. Takamura, M. Uehara, J. Suzuki, K. Sekine, K. Tamura, J. Power Sources 158 (2006) 1401–1404.
[28] M. Yoshio, T. Tsumura, N. Dimov, J. Power Sources 146 (2005) 10–14.
[29] W.-J. Zhang, J. Power Sources 196 (2011) 13–24.
[30] H. Wang, T. Abe, S. Maruyama, Y. Iriyama, Z. Ogumi, K. Yoshikawa, Adv. Mater. 17 (2005) 2857–2860.
[31] X.H.X.Y.Y. Tang, Y.X. Yu, S.J. Shi, J. Chen, Y.Q. Zhang, J.P. Tu, Electrochim. Acta 88 (2013) 664.
[32] C. Pereira-Nabais, J. Światowska, A. Chagnes, F. Ozanam, A. Gohier, P. Tran-Van, C.-S. Cojocaru, M. Cassir, P. Marcus, Appl. Surf. Sci. 266 (2013) 5–16.
[33] J.S. Catarina Pereira-Nabais, Alexandre Chagnes, Appl. Surf. Sci. 55 (2013) 5.
[34] T.D. Hatchard, J.R. Dahn, J. Electrochem. Soc. 151 (2004) A838–A842.
[35] J. Saint, M. Morcrette, D. Larcher, L. Laffont, S. Beattie, J.P. Pérès, D. Talaga, M. Couzi, J.M. Tarascon, Adv. Funct. Mater. 17 (2007) 1765–1774.
[36] M. Yoshio, H. Wang, K. Fukuda, T. Umeno, N. Dimov, Z. Ogumi, J. Electrochem. Soc. 149 (2002) A1598.
[37] P. Verma, P. Maire, P. Novák, Electrochim. Acta 55 (2010) 6332–6341.
[38] Ge Ji, Yue Ma, Jim Yang Lee, J. Mater. Chem. 21 (2011) 9819.
[39] T. Jiang, S. Zhang, X. Qiu, W. Zhu, L. Chen, Electrochem. Commun. 9 (2007) 930–934.
[40] S.S.H. Riccardo ruffo, Candace K. Chan, Robert A. Huggins, Yi Cui, J. Phys. Chem. 113 (2009) 11390.
[41] X. Wang, Z. Wen, Y. Liu, Y. Huang, T.-L. Wen, Solid State Ionics 192 (2011) 330–334.